Use of 3D Potential Field and an Enhanced Breadth-first Search Algorithms for the Path Planning of Microdevices Propelled in the Cardiovascular System

Wael Sabra, Matthew Khouzam, and Sylvain Martel*

NanoRobotics Laboratory, Department of Computer Engineering and Institute of Biomedical Engineering,
École Polytechnique de Montréal (EPM), Campus of the Université de Montréal, Montréal (Québec) Canada

*E-mail: sylvain.martel@polymtl.ca URL: www.nano.polymtl.ca

***Abstract*—Potential field algorithms often used in path finding applications on a 2D plane are expanded onto a 3D map trajectories for navigation planning of a microdevice designed to be propelled through the cardiovascular system using magnetic gradients generated by a clinical MRI system. This system assembles a 3D reconstruction of a cardiovascular system through magnetic resonance angiography images. The method also allows the extraction of the physiological properties of the given network.**

Keywords—**Image processing, magnetic resonance imagery, angiogram, DICOM, microsurgery, local minima, potential field, wave propagation, path planning**

I. Introduction

The MR-Sub (Magnetic Resonance Submarine) project showed that magnetic gradients generated from a clinical Magnetic Resonance Imaging (MRI) system could propel a ferromagnetic core in blood [1-5]. These preliminary results suggest that special microdevices could be designed to be propelled, tracked, and controlled in the human body and especially in the blood circulatory system. This approach allows more sites to become accessible in order to perform specific medical tasks. This method aims at complementing or replacing for simpler tasks, catheters in many sites in the human body that are still inaccessible or at high risks with more conventional instruments where possible encumbrance of the blood vessels and tissue damages caused by friction especially for complex pathways may be a concern.

The propulsion of such microdevices is very complex. It depends on many factors and as such, it is essential to provide a software tool that will assist in determining the best locations to inject a microdevice and the best appropriate paths to automatically guide such microdevice through the cardiovascular system to the target location. As such, the proposed software tool must also have a user interface capable of visualizing the blood vessels and extracting information from the blood vessels.

To accomplish such tasks, the potential field (PF) algorithm [6] is considered. Until now, the potential field algorithm has been mostly used in 2D robotics and control applications but the method can evolve onto a 3D workspace such as the cardiovascular system. This would allow path planning (with three degrees of freedom) prior to navigate such microdevices in the blood vessels. This paper describes the current work on the path finding, reconstruction and visualization software in the context of the MR-Sub project.

II. Constraints

The proposed method described here, will be expanded to consider several constraints as well as physiological and technical issues. For instance, the propulsion force induced on the microdevice depends on the material properties of the embedded ferromagnetic core and its overall size. As such, the path planning algorithm must ensure that such induced force is sufficient to counteract the reciprocal blood flow which is typically higher in larger diameter blood vessels. Furthermore, the ratio between the diameter of the microdevice and the diameter of blood vessel being used must be within a specified range (~0.23-0.57, assuming a spherical shape) [5]. For instance, if the ferromagnetic core is too small relative to the diameter of the blood vessel, not enough propulsion force will be induced resulting to a loss of control of the microdevice. Similarly, if the diameter of the microdevice is too large, the risk of obstruction will increase. In both situations, serious consequences to the patient health may occur. The shape of the microdevice will influence the drag force which must be known and considered by the path planning software. Other factors such as buoyancy, blood viscosity, amplitudes of contraction of the vessels, etc., must also be taken into account for maximum security and reliability.

In this paper, constraints related to MR-imaging have been considered. For instance, an MRI system [7] takes multiple images sequentially. Due to the fact that the body is in motion, there may be discontinuities between two images generated by these motion artifacts. Furthermore, an image may not be verifiable using blood doping methods [7] since the bolus agent used to highlight the blood breaks down in a matter of minutes. Angiographic images may not be complete; some methods will only detect the blood flow in one direction. Moreover, in order to avoid clipping or data loss in the areas of interest, the entire spectrum of available intensity is not used. To reduce the time required for the procedure, interlaced images are often used instead of

Preprint submitted to 27th IEEE EMBS Annual International Conference.
Received April 8, 2005.

recording images continuously. Since of all these issues, development has been more focused on cone-beam CT scanners. The MR images use the DICOM standard [8, 9]. These files contain image and network information not available with standard image files, such as the physical dimensions of a pixel, the number of the slice of the image and the characteristics of the MRI system. These parameters provide every pixel an absolute X, Y and Z position. The images are defined using a 12-bit depth grayscale. Each pixel has a volume (typically 1 mm^3) and can be viewed as voxels which can be considered as a node in the present methods. These voxels are sometimes larger than the microdevice or the blood vessels the angiographic images still need parsing. These images are not saturated and hence, need to be enhanced. Since precision is an essential factor, the amount of image filtering is also minimized.

Another issue that complicates the implementation of such a software tool is the complexity of the blood vessel network as it is riddled with forks, with changes in volume due to contractions of the blood vessels, and contains local minimums. More specifically, these minimums consist of points that appear as dead-ends for the proposed algorithm.

III. Reconstruction and Visualization

An MRI system generates slice images of a specific zone. In order to set up a 3D volume of the images, the images are parsed and relevant information is extracted. Once the images are reconstructed, the 3D data structures and filters may be applied to the whole volume. The filters used are normalization, static thresholds, dynamic thresholds and convolution matrices. The normalization filter minimizes the precision loss incurred by applying other filters and compensates for missing frames or missing regions in the data source. The static thresholds allow the rough detection of blood vessels in an angiogram. The dynamic filtering allows a more sensitive detection of blood vessels but generates more false positive results since it is sensitive to high frequency noise. The previous two methods are used to address the issues of varying angiogram intensities for blood vessels. The convolution matrix functionalities allow the image to be filtered and enhanced. These filters include tools such as edge detection, Gaussian blurs, median blurs and sharpen mask options [10]. A program has been developed to image the 3D structure. It allows instant feedback to the user and verifies if the precision obtained is still acceptable after filtering. This visualization and filtering toolkit allows users to program analytical algorithms without having to deal with DICOM-based medical images. Hence, with higher levels of abstraction, the development and validation of complex algorithms is made easier.

IV. Path Finding and Property Extraction

The choice of the algorithm requires a review of current path finding techniques. It should be specified first that the best path through the cardiovascular network is not necessarily the shortest path or the fastest path. It depends on the conditions specific to each network such as neighboring organs, difficult curves and possible obstructions.

There are two main categories of path-finding algorithms, local algorithms and global algorithms. Local algorithms do not retain a memory of the whole map and only provide the path considered the best. Global algorithms have the advantage of knowing the whole map at any given time at the cost of being usually much more memory intensive.

The criteria for the best algorithm are computation time, memory usage, local minima handling, and the capability of determining multiple paths. Local minima handling is necessary since the blood vessels seen as paths present local minimums. Multiple path capabilities are necessary in order to offer to the operator, multiple alternative paths to reach a target.

TABLE I
Review of existing algorithms

Algorithms	Time complexity	Space complexity	Multiple-Paths
Breadth-First Search	$O(k^n)$	$O(k^n)$	yes
Depth-First Search	$O(k^m)$	O(km)	no
Random Tree	Random	Random	no
Dijkstra	Depends	Depends	yes
Best-First Search	Depends	Depends	No
A*	$O(k^n)$	$O(k^n)$	No
Cellular decomposition	O(NlogN)	O (N)	No
Skeletal	Depends	Depends	Yes
2D Potential fields[5]	Depends	Depends	No

k= branching factor, n = average depth, m=maximum depth, N= number of nodes.

In Table 1, k is the branching factor, the amount a graph will spread out, n is the average depth of the graph, m is the maximal depth of a branch of the graph and N is the number of nodes in the given graph, typically k*n.

After reviewing all the algorithms listed in Table 1, the best choice for this application appears to be the breadth-first search. For example, the method “depth-first search” (see Table 1) will end at the first match and therefore it will not guarantee the best path while the “best-first search” on the other hand, will end at local minima, and the A* will not handle multiple paths. Nonetheless, an interesting feature of the PF algorithm is the extraction of characteristics about the

Preprint submitted to 27th IEEE EMBS Annual International Conference.
Received April 8, 2005.

graph by highlighting obstacles and creating a topographical map of the region of interest. It also adapts well to a changing graph. These features address the issues of the movements of a patient and the capability for selecting a proper blood vessel within the identified physiological and technical constraints (Sect. II). Therefore, for the purposes of this project, a hybrid method consisting of the PF and breadth-first search is proposed.

The proposed PF algorithm is based on Newton's law of attraction as depicted in (1).

$$F_{obstacle} \approx \frac{M_1 M_2}{d^2} \quad (1)$$

The value of a potential at a given point is equal to the sum of the forces of repulsion (2).

$$PF(x,y,z) = \sum F_{obstacles} \quad (2)$$

In Eq. 2, M_1 and M_2 are constants. Equation 3 is the result of substituting (1) in (2).

$$PF(x,y,z) = \sum \frac{cte}{d^2} \quad (3)$$

Potential field is used initially to create a force map of the region of interest. It first creates a list of obstacles and then, it calculates the sum of the squared distance from each obstacle to the voxel. The result represents the effect or cost of each obstacle in a given voxel. Such force on all three axes, decreases by a $1/d^2$ where d is the distance between the microdevice and a particular obstacle.

The breadth-first search which can be represented as a wave traveling through the topological force map from the source to the destination is then applied to the force map. This phase shows all the available paths thus addressing the multiple-path requirement. The method is limited to a maximum distance through parameters in the software to restrict the number of potential paths. The pseudo-code for the algorithm is described at the end of the paper.

Fig.1a and Fig.1b illustrate the behavior of the PF algorithm. The images represent 2D slices of a 3D region of interest. Fig. 1 (a) shows the degradation of a PF. The darker squares are further away from a punctual obstacle in a blood vessel. Fig. 1 (b) shows the behavior of the PF algorithm in a closed surface. This is comparable to a transversal slice of a blood vessel. Here for the sake of clarity in the images, the attenuation is 1/d and not $1/d^2$ since squared degradation in the map would generate insignificant differences after 2 iterations.

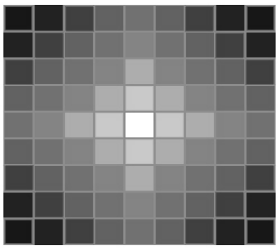

(a)

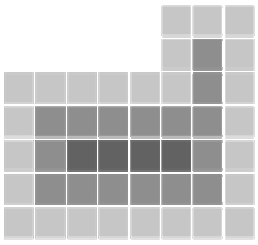

(b)

Fig.1. (a) 2D slice visualization of the potential field of a punctual obstacle and (b) transversal slice of a blood vessel.

The breadth-first search algorithm, in conjunction with the PF algorithm generates the candidate paths to be taken by a microdevice while the PF is given as a cost element to each step in the search. The paths returned show the cost of each step and thus, pertinent information such as path length, mean path width, largest point, narrowest point and an estimated travel time.

V. Results

The MRI test bench was run on a sample interlaced matrix containing the angiogram of a human brain. The static threshold was set at 50% in Fig. 2a and at 35% in Fig. 2b. The previous image was also passed though a "sharpen" convolution matrix and was displayed using smooth shading.

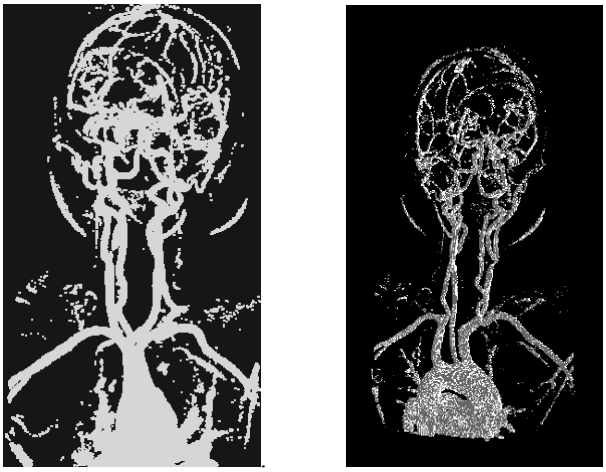

(a) (b)

Fig.2. 3D volume reconstruction from upper half MRI images of a human body (a) by using a static threshold of 50%and (b) by using a static threshold of 35% with a convolution matrix.

The PF algorithm was coded and simulated in MATLAB. A 2D slice of a 3D image is plotted in a height map as depicted in Fig. 3 and Fig. 4. Fig. 3 is the result of applying the PF algorithm on a region of interest containing 2 null dimension (point) obstacles.

Preprint submitted to 27th IEEE EMBS Annual International Conference.
Received April 8, 2005.

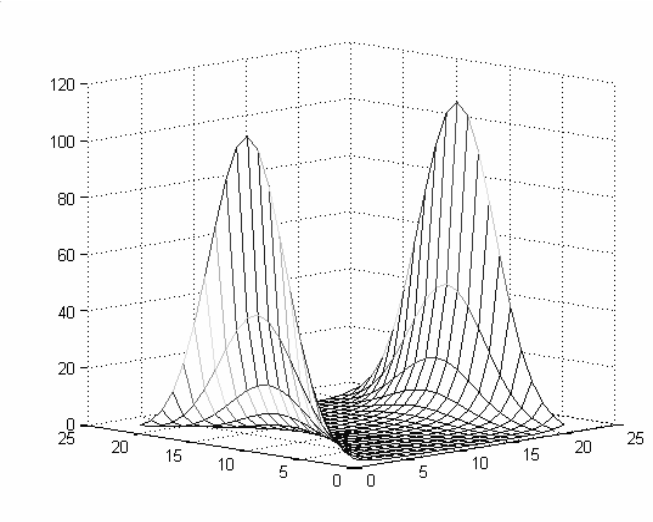

Fig.3. Two-point PF simulation on a 2D plane

The results plotted in Fig. 4 use the same simulation as the one shown in Fig. 3 but with two parallel straight lines obstacles.

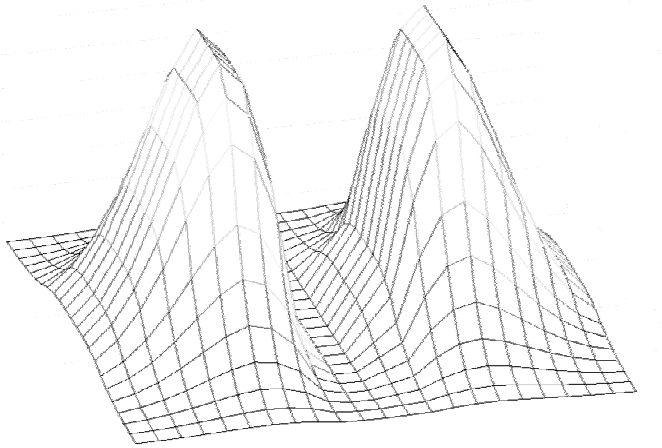

Fig.4. Potential field simulation of the 2D input slice of a center sliced blood vessel.

VI. Discussion

The preliminary results of the toolkit show that the threshold function alone is sufficient for most normalized angiograms. The convolution matrix functionalities can solve the remaining problems but could be omitted in many cases since they increase the memory requirements by up to 2700%. This is due to the convolution matrix storing multiple copies of the structure in order to preserve the dependencies in the order of transformations.

A 3D network created from the sparse data source, a source missing some elements, can be interpolated. The generated images did have some threshold detection problems with the dynamic filter as the high frequency signals were not preserved.

The performance of the display system with most 3D functionalities disabled was acceptable on older PCs. This will allow a wider developer base.

The implemented 3D breadth-first search algorithm has removed the local minima issue while efficiently finding the best path as defined by the costing of the PF. All of the addressed requirements have been satisfied. Characteristics are extracted and a topographical pressure map is generated which allow better navigation of a microdevice through blood vessels. The images illustrate the functionality of the PF algorithm. Fig. 4 illustrates a path drawn between two discrete obstacles. The farther away a cursor is, the less it will be repelled by the forces of the obstacles. It shows the algorithm interpreting a blood vessel where the two peaks are the walls of the vessel and the valley in the center is an area where the microdevice may travel.

VII. Conclusion

The results show the feasibility of implementing a 3D algorithm for path-planning for a microdevice to be propelled through the blood vessels by magnetic gradients generated by an MRI system. An issue with this system is that the potential fields will be very weak far from the blood vessels, so if there are any discontinuities in the initial MRI images, the system could bypass the blood vessels all together and plot a path in the wrong areas. However, the convolution matrix filters correct this issue. Moreover, the breadth-first search algorithm has a requirement in its path finding logic to always pick a passage with a maximal diameter. Sending the images from an MRI system onto a 3D structure and using an advanced potential field algorithm has fulfilled the goal and may prove to be an important tool in the context of the MR-Sub project. Nonetheless, additional work needs to be done to consider several physiological and technological constraints as mentioned briefly in the paper.

Acknowledgment

This work is supported by a strategic grant from the Natural Sciences and Engineering Research Council of Canada (NSERC) and in part by a Canada Research Chair (CRC) in Conception, Fabrication, and Validation of Micro/Nanosystems, the Canadian Foundation for Innovation (CFI), and the Government of Québec. We acknowledge the support of Hôpital Notre-Dame and Centre Hospitalier de l'Université de Montréal (CHUM) that provided the infrastructure to conduct MRI tests.

Preprint submitted to 27th IEEE EMBS Annual International Conference.
Received April 8, 2005.

REFERENCES

[1] J-B. Mathieu, S. Martel, L. Yahia, G. Soulez, and G. Beaudoin, "Preliminary studies for using magnetic resonance imaging systems as a mean of propulsion for microrobots in blood vessels and evaluation of ferromagnetic artefacts," Canadian Congress on Electric and Computer Engineering, Montreal, Canada, p 835-838, 2003.

[2] J-B. Mathieu, S. Martel, L. Yahia, G. Soulez, and G. Beaudoin, "MRI systems as a mean of propulsion for a microdevice in blood vessels," *Proceedings of the IEEE-EMBS Conf. on Biomedical Eng.*, Vol. 4, pp. 3419-3422, Sept. 2003.

[3] S. Martel, J-B. Mathieu, O. Felfoul, H. Macicior, G. Beaudoin, G. Soulez, and L'H. Yahia, "Adapting MRI systems to propel and guide microdevices in the human blood circulatory system*", Proceedings of the IEEE-EMBS Conf. on Biomedical Eng.*, Sept. 2004, pp. 1044-1047.

[4] J-B. Mathieu, S. Martel, L'H. Yahia, G. Soulez, and G. Beaudoin, "Preliminary investigation of the feasibility of magnetic propulsion for future microdevices in blood vessels," *Bio-Medical Materials and Eng.*, 2005 (accepted)

[5] J-B. Mathieu, G. Beaudoin, and S. Martel, "Method of propulsion of a ferromagnetic core in the cardiovascular system through magnetic gradients generated by an MRI system," *IEEE Trans. on Biomedical Eng.*, 2005 (in review)

[6] J. Barraquand, B. Langlois, and J.C. Latombe, "Numerical Potential Field Techniques for Robot Path Planning," IEEE Trans. on Systems, Man and Cybernetics, 22(2), 224-241, 1992.

[7] Kim S-G, "Quantification of relative blood flow change by flow-sensitive alternating inversion recovery (FAIR) technique: application to functional mapping," *Magn. Reson. Med.* 34:293–301, 1995.

[8] http://medical.nema.org/dicom/2004.html

[9] http://dicom.offis.de/

[10] M. Hopf and T. Ertl, "Accelerating 3D convolution using graphics hardware". In *Proc. Of IEEE Vis '99*, pages 471–474, 1999.

PSEUDOCODES OF THE ALGORITHM

```
point start, destination;

% Find obstacles
list<point> Obstacles := empty;
foreach(Point in region_of_interest)
        if Point = obstacle then
                Obstacles.insert(Point) ;
        end_if
        Point.intensity := 0;
end foreach

% Create potential fields map
foreach Point in region_of_interest
  foreach obstacle in list
        Point.intesity :=
          Point.intensity + dst(Point, obstacle)^-2
  end foreach
end foreach

% Find Paths
tree<point> map;
list<node> ends;
list<list<point>> paths;
map.root(destination);
populate(map);
ends := find(start in map);

foreach Point in ends
  paths.insert( list(end to beginning));
end foreach

foreach path in paths
  getStatistics(path);
end foreach
```

Preprint submitted to 27th IEEE EMBS Annual International Conference.
Received April 8, 2005.